Pure Appl. Chem., Vol. 76, No. 3, pp. 625–633, 2004.

New insights into the mechanism of molybdenum-catalyzed asymmetric alkylation*

Shane W. Krska[1,‡], David L. Hughes[1], Robert A. Reamer[1], David J. Mathre[1], Michael Palucki[1], Nobuyoshi Yasuda[1], Yongkui Sun[1], and Barry M. Trost[2]

[1]Department of Process Research, Merck and Co., Inc., Rahway, NJ 07065, USA; [2]Department of Chemistry, Stanford University, Palo Alto, CA 94305-5080, USA

Abstract: The major features of the catalytic cycle, including structures of key intermediates, have been determined for the molybdenum-catalyzed asymmetric alkylation. The crystal structure of the π-allyl intermediate exhibits 3-point binding of an anionic ligand. Based on NMR analysis, this species adopts in solution a structure consistent with that observed in the solid state. For the allylic alkylation, the crystal structure predicts the opposite stereochemistry vs. that observed experimentally, which suggests that either the reaction proceeds via a minor isomer (Curtin–Hammett conditions) or with retention of configuration. In addition, CO transfer, promoted by $Mo(CO)_6$, has been found to play a key role in catalyst turnover.

INTRODUCTION

Molybdenum-catalyzed asymmetric allylic alkylation reactions in recent years have emerged as a powerful tool in organic synthesis, providing regiochemistry that is complementary to that seen with Pd [1] (eq. 1). A number of ligands have now been successfully designed for this reaction [2–6], and reports of synthetic applications have begun to appear [7,8].

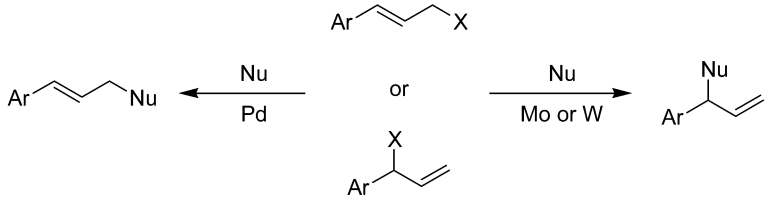

(1)

Interest at Merck arose in this reaction while searching for an efficient route to cyclopentanone **1**, an intermediate in the synthesis of one of our development candidates (Scheme 1). We found the key asymmetric center could be incorporated using the Mo-catalyzed asymmetric alkylation with bis-picolinamide ligand **6** [3] using **2b** as substrate [7]. Using this method, enantioselectivies as high as 97 % ee could be obtained, with selectivity for the branched product vs. the linear of 19:1.

*Plenary and invited lectures presented at the 12th IUPAC International Symposium on Organometallic Chemistry Directed Towards Organic Synthesis (OMCOS-12), Toronto, Ontario, Canada, 6–10 July 2003. Other presentations are published in this issue, pp. 453–695.

‡Corresponding author

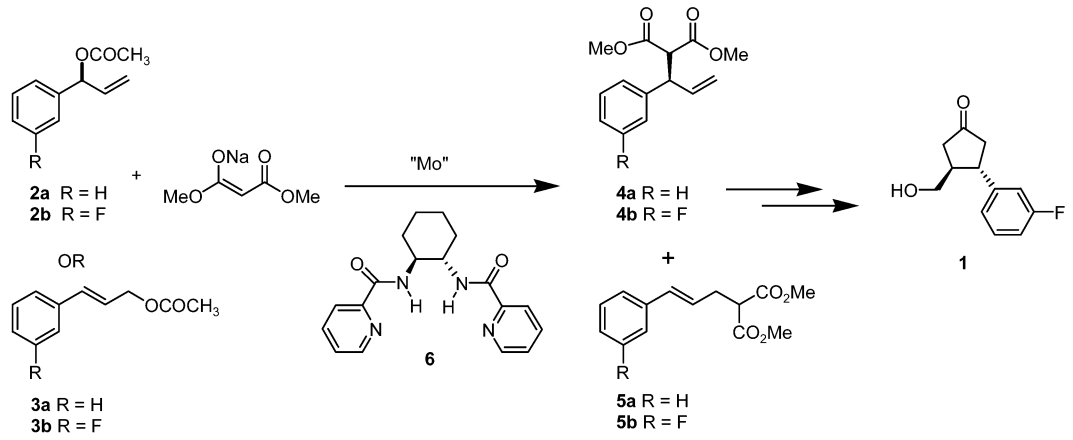

Scheme 1

During the course of this work, it was discovered that $Mo(CO)_6$ could be used as a cheap, readily available Mo precatalyst for this reaction in place of the more traditionally used $Mo(CO)_3$(cycloheptatriene) or $Mo(CO)_3(EtCN)_3$ [6a,9]. When appropriately activated, $Mo(CO)_6$ gave comparable yields, ee's, and branched/linear (b/l) ratios relative to the other two Mo precatalysts for a number of substrates. This led us to conclude that all three precatalysts were generating the same catalytic species [9].

The question became, then, what was the nature of this catalytic species? One of the authors proposed a number of possible structures in his original communication of Mo-catalyzed asymmetric alkylation using ligand **6** [3a]. When we started the present work, no definitive structural studies had been published with ligands analogous to **6**. However, in late 2001 Pfaltz published the crystal structure of **7**, a tricarbonylmolybdenum(0) complex of a bis(dihydrooxazole) ligand analogous to **6** [5b] (Scheme 2). In this complex, the ligand binds in a facial, tridentate fashion through the two dihydrooxazole nitrogen atoms and one of the adjacent amide carbonyl oxygen atoms, suggesting the potential involvement of at least three donor sites in the ligand. Work published by Kočovský that same year, as well as unpublished work in the laboratory of one of the authors, showed that analogs of ligand **8** lacking either a second remote pyridine or amide functionality exhibit markedly reduced activity in molybdenum-catalyzed asymmetric alkylation reactions compared to the parent ligand, further supporting the notion that tridentate ligand binding is important for catalytic activity [4a].

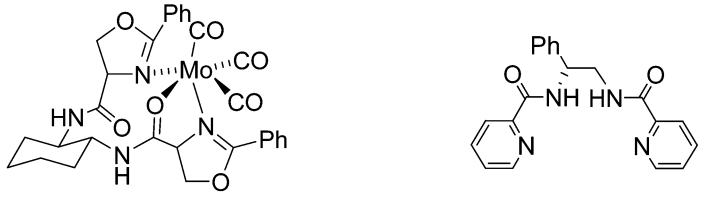

Scheme 2

LIGAND BINDING STUDIES

A more in-depth study of the binding mode of ligand **6**, similar in approach to the work described above, was carried out by preparing a number of derivatives of ligand **6** and comparing their activities

and selectivities to that of **6** under standard molybdenum-catalyzed alkylation reaction conditions (Scheme 1) [10]. Three representative ligands from this study are shown in Scheme 3 below.

Picolinamide-benzamide ligand **9** showed superior selectivity to **6** in the reaction of linear carbonate **3a** with malonate (99 % ee, b/l = 60), although the reactivity was reduced by approximately 50 %. This is in contrast with the results discussed above for ligand **8**, wherein replacement of one of the pyridine groups with phenyl resulted in almost no catalytic activity. The bis-phenyl ligand **10** had very low activity and produced an ee of only 24 %, indicating that binding only via the two amides, if occurring, provided a poor asymmetric catalyst. Methylation of both amide groups of **6** to give ligand **11** resulted in almost no catalytic activity, suggesting the possibility that deprotonation of one or more amides was occurring under the basic conditions of the reaction.

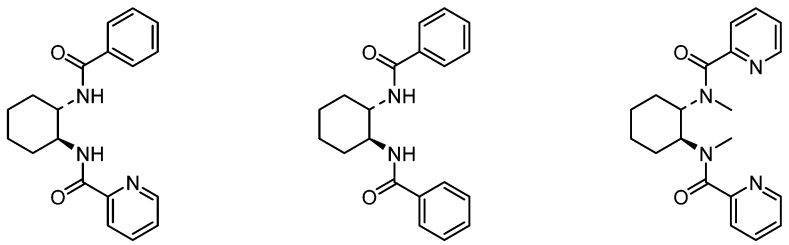

Scheme 3

The studies described above established that only one of the pyridine groups in ligand **6** was required for effective catalysis. This fact, along with the potential for ligand **6** to bind more than one Mo center [11], prompted us to choose ligand **9** for more in-depth spectroscopic studies [12].

The reaction of ligand **9** with (NBD)Mo(CO)$_4$ produces complex **12**, with 2-point binding through the pyridine nitrogen and amide group (Scheme 4). This neutral Mo-ligand complex reacts with either branched or linear carbonates in THF (at room temperature and 50 °C, respectively) to form π-allyl complex **13**. The stoichiometry of this reaction, as determined by NMR, involves formation of 1 equiv each of **13**, MeOH and free ligand from 2 equiv of complex **12**. In addition, a significant amount (presumably 1 equiv) of Mo(CO)$_6$ is observed by ^{13}C NMR spectroscopy. The methanol observed is formed, along with CO_2, from the methyl carbonate leaving group upon deprotonation of one of the

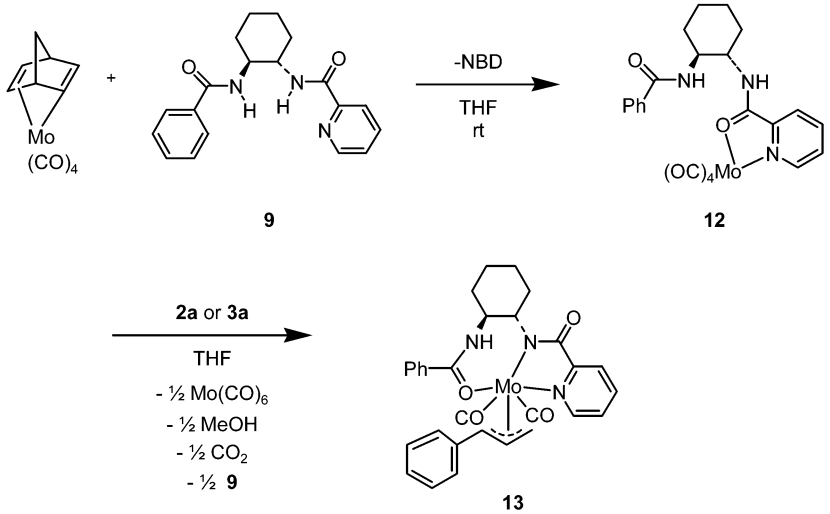

Scheme 4

amide groups of the ligand; the resulting anionic ligand ultimately becomes a part of the π-allyl complex **13**.

A suitable crystal of the π-allyl complex **13** was grown, and the X-ray structure is shown in Fig. 1. Noteworthy features of this structure include the following: (1) the allyl moiety binds in a η^3 fashion to Mo, with one face clearly open for reaction with a nucleophile; (2) the ligand coordinates to the metal via three-point binding: the pyridine nitrogen, the nitrogen of the deprotonated amide, and the carbonyl oxygen of the undeprotonated amide; and (3) the complex contains two CO ligands. The overall geometry of the complex, including the *syn* orientation of the allyl moiety with respect to the CO ligands, is similar to other structurally characterized $L_2(CO)_2XMo(\eta^3$-allyl) complexes [13].

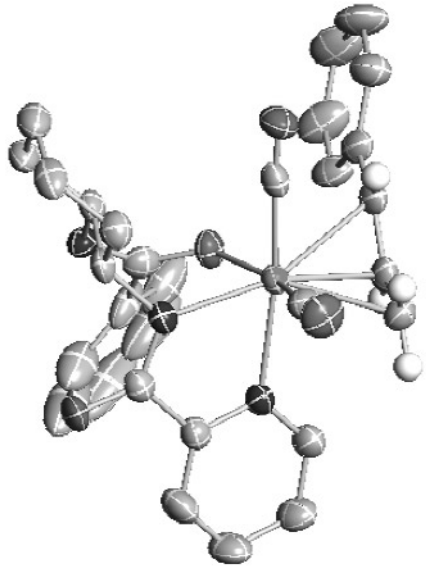

Fig. 1 Crystal structure of π-allyl complex **13**. Thermal ellipsoids are drawn at the 50 % probability level. Solvent (THF) and non-allylic H atoms are omitted for clarity.

The solution structure of **13** was studied by multinuclear NMR, including nuclear Overhauser effect (NOE) measurements [10]. The results were consistent with either one of two structures (Δ ***si*** or Λ ***re***) illustrated in Scheme 5 (wherein py represents the pyridine moiety of **9**, N represents the deprotonated picolinamide nitrogen, and O represents the coordinated benzamide carbonyl). Both structures exhibit three-point binding of the chiral ligand, but with different stereochemistry about the octahedral Mo center (defined, for purposes of this discussion, as Δ vs. Λ) and different faces of the π-allyl moiety (*re* vs. *si*) bound to Mo. These two structures are pseudo-enantiomers of each other, with inverted

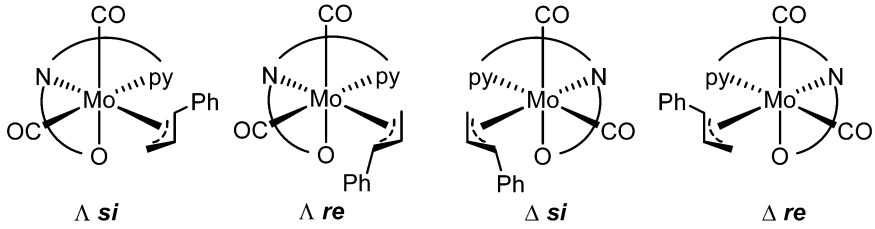

Scheme 5

stereochemistry at Mo and the allyl fragment, but the same configuration of chiral ligand. The Δ ***si*** structure corresponds to that seen in the solid state.

Solution NMR studies also revealed the presence of a minor π-allyl complex in solution, in dynamic equilibrium with the major species, present in ~1 % abundance. Spin saturation transfer experiments demonstrated that this species was not related to **13** via a π-σ-π isomerization mechanism, since there was no observed exchange of *syn* and *anti* protons on the terminal allyl carbon. In addition, the allyl moiety in this complex is in the W conformation, as with **13**. It is likely that this species is related to **13** via a Δ-Λ flip of the chiral ligand, giving complex Λ ***si*** (assuming the major species in solution is Δ ***si***). However, the low abundance of this species in solution precluded a definitive assignment of its structure.

Overall, the ligand binding studies confirmed earlier indications that tridentate coordination was an important feature of this class of ligands, and that at least one of the amide nitrogens was deprotonated under the reaction conditions. The most surprising feature of the solid-state structure was the observation that although one face of the π-allyl moiety is clearly open for approach of a nucleophile, attack of malonate in this direction predicts stereochemistry opposite to that which is observed in the overall catalytic reaction. It is possible that the most stable species in solution is not the same as that which crystallizes, i.e., that the Δ ***si*** complex observed in the solid state is converted upon dissolution to the Λ ***re*** complex via a π-σ-π isomerization of the allyl moiety and a Δ-Λ flip of the chiral ligand. However, given the lack of observation of any minor isomers in solution related to the major species via π-σ-π isomerization, this seems unlikely.

Assuming the major species in solution is the same as that observed in the solid state (the Δ ***si*** isomer), then either this is not the reactive species, i.e., the reaction is occurring through a minor, unobserved **(**Δ **or** Λ**)** ***re*** isomer derived from the major species via π-σ-π isomerization, or the nucleophilic displacement reaction with malonate is occurring with retention of configuration. It is well known that allylic alkylation reactions catalyzed by Pd occur with inversion of configuration in both the oxidative addition and nucleophilic displacement steps, giving overall retention of configuration [14]. In the case of Mo, the reaction proceeds with overall retention [3], but the stereochemistry of each step in the reaction has not been definitively elucidated. A few studies have shown that stoichiometric oxidative additions with Mo can occur with retention [15], and Kočovský reported a Mo-catalyzed allylic alkylation of a constrained system that is best explained by a retention–retention mechanism [16]. Clearly, more experimental work will be required to understand the intimate mechanism of the oxidative addition and nucleophilic displacement steps of this reaction.

It is useful to mention in this regard the kinetic resolution and memory effects associated with this reaction [17]. The two enantiomers of branched carbonate **2a** exhibit marked differences in reactivity using ligand **6**, with the *S*-enantiomer reacting ~10× faster than the *R*, and giving much higher ee (99 vs. 70 % with *R*-carbonate). Scheme 6 shows a model that rationalizes this observation. This model employs equilibrating diastereomeric π-allyl intermediates **A** and **A-dia** in which the rate of nucleophilic attack is competitive with the rate of equilibration. The scheme shows both oxidative addition and nucleophilic displacement as occurring with retention of configuration, although the model would be equally valid if both occurred with inversion. Since the diastereomer equilibration is (formally) a unimolecular process, and the nucleophilic substitution is bimolecular, the effect of [malonate] on the enantioselectivity of the reaction provides a useful mechanistic tool for studying these reactions.

According to the model shown above, the memory effect seen with the slower reacting *R*-carbonate isomer arises from fast nucleophilic displacement occurring with **A-dia** to give the minor product enantiomer, competitive with the rate of equilibration of **A-dia** to **A** and subsequent trapping with malonate to form the major product enantiomer. Thus, the model predicts an increase in enantioselectivity with the slow-reacting *R*-carbonate when [malonate] is kept low. Indeed, adding malonate slowly over 6 h to an otherwise typical reaction results in an increase in ee from 70 to 92 %. Conversely, decreasing [malonate] ought to have the effect of lowering the enantioselectivity with the fast-reacting

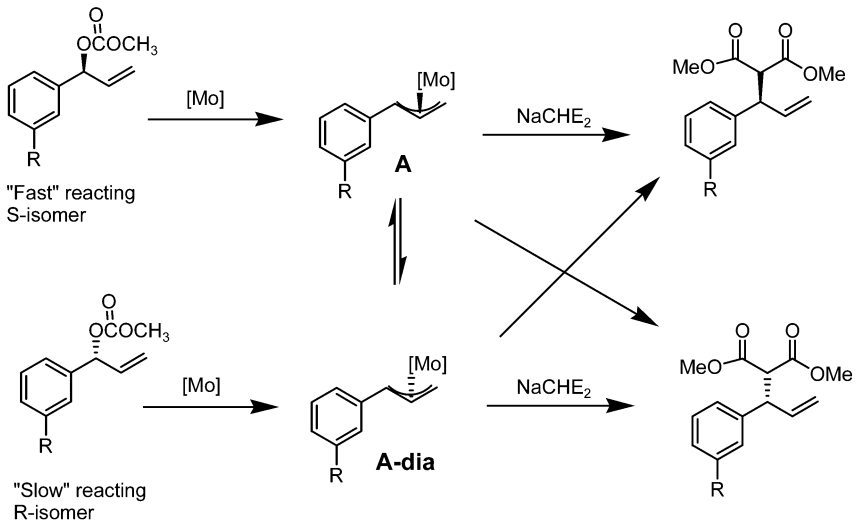

Scheme 6

S-enantiomer. Experimentally, this is what is observed, as the ee drops from 97 % ee at 0.6 M malonate to 92 % ee at 0.07 M malonate.

These results are consistent with the mechanistic picture in Scheme 6 in which the *R*- and *S*-carbonates form different diastereomeric allyl complex intermediates **A** and **A-dia** that lead, respectively, to the major and minor product enantiomers. However, the results are not conclusive as to which intermediate, **A** or **A-dia**, is more stable, nor do they imply whether the reaction proceeds by a retention–retention or an inversion–inversion mechanism. Further experimental work will be required to answer these intriguing questions.

REACTIVITY STUDIES

In order to gain more insight into the mechanism of the reaction, we undertook reactivity studies of the allyl complex in an attempt to model the basic steps of the catalytic cycle. When π-allyl intermediate **13** was generated in solution from complex **12** and the allylic carbonate **3a**, it reacted cleanly with sodium dimethyl malonate ($NaCHE_2$) to form the substituted malonate product with an ee of >95 %. However, when the isolated crystals of complex **13** were redissolved in THF and combined with $NaCHE_2$, surprisingly no reaction occurred. Reasoning that the difference in reactivity was due to the presence of one or more of the by-products of formation of the allyl complex (Scheme 4), we repeated the reaction between isolated **13** and $NaCHE_2$ in the presence of excess $Mo(CO)_6$ (eq. 2). This time, the product **4a** was cleanly generated in 82 % yield and >95 % ee according to NMR spectroscopy. The role of the added $Mo(CO)_6$ became apparent upon identification of the Mo-containing product of this reaction as tetracarbonylmolybdate complex **14** [12]. In essence, $Mo(CO)_6$ was acting as a CO donor, providing **13** with the necessary additional CO ligands to function as a leaving group in the nucleophilic addition of malonate to the coordinated allyl moiety.

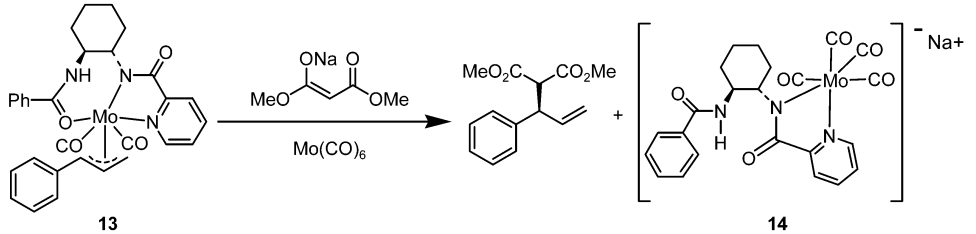

(2)

Complex **14** can be prepared by reaction of complex **12** with NaH or $NaCHE_2$. For isolation purposes, it was prepared from NaH. Isolated **14** reacts with either branched or linear carbonates **2a** or **3a** to regenerate **13**. Importantly, both enantiomers of **2a** give the same complex **13** in high yield. Putting together the reactivity shown in Schemes 4 and 7, one can construct the essential outline of the catalytic cycle for the Mo-catalyzed asymmetric alkylation (Scheme 7). Precatalyst **12** reacts with carbonate **3a** to generate π-allyl complex **13** according to Scheme 4. Complex **13** reacts with malonate in the presence of a CO source [either **14** or $Mo(CO)_6$] to form product **4a** and molybdate complex **14**. Complex **14** reacts with carbonate **3a** to regenerate complex **13** and release CO. A typical synthetic experiment using catalytic molybdenum was followed by NMR, and complexes **13** and **14** were the only Mo-containing species observed, with high mass balance in Mo conserved throughout the reaction. This confirms that **13** and **14** are the catalyst resting states under actual catalytic synthetic conditions.

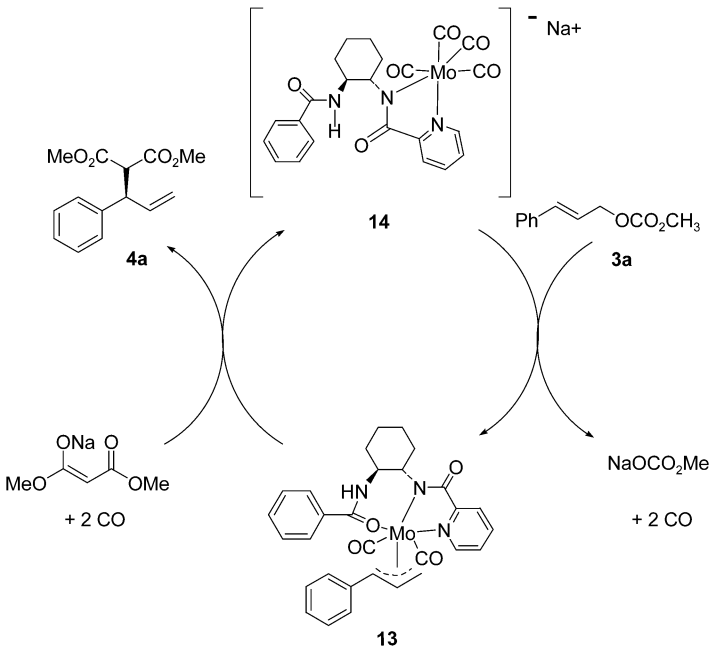

Scheme 7

With the broad outlines of the catalytic cycle in place, we return to the question of the nature of the reactive species. The results of the reactivity studies described above suggest a reactive Mo-allyl species bearing >2 CO ligands. Two plausible structures for such a complex may be drawn, either an η^1-allyl complex **15** or π-allyl complex **16** in which the hemi-labile benzamide carbonyl moiety has been displaced by the more strongly binding CO ligand (Scheme 8). It may be that both complexes are viable intermediates, and exist in equilibrium with each other as part of the π-σ-π equilibration of the

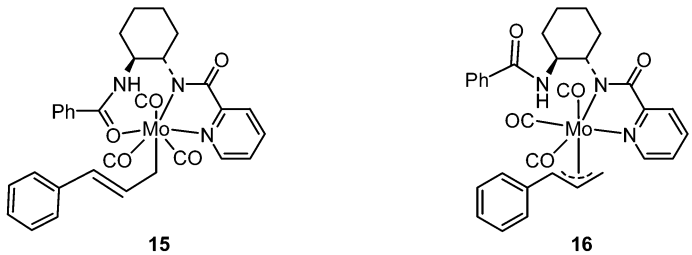

Scheme 8

two π-allyl facial isomers. So far, attempts to observe these species by reacting **13** with excess $Mo(CO)_6$ or CO(g) have not been successful. We are currently pursuing other approaches, including kinetic and theoretical studies, to answering this and other open questions about this fascinating system.

SUMMARY

Designed ligand probes, spectroscopic studies and isolation of key catalyst resting states have all provided new insight into the mechanism of the Mo-catalyzed asymmetric alkylation reaction. Ligand probe studies revealed that picolinamide-benzamide ligand **9** gives yields, enantioselectivities and b/l ratios in the allylic alkylation reaction that are comparable to, or better than, the parent ligand **6**. The Mo π-allyl complex **13** derived from **9** and the methyl carbonate of cinnamyl alcohol was isolated and fully characterized. Its X-ray crystal structure is characterized by three-point binding of the chiral ligand, consistent with previous postulates in the literature. The crystal structure predicts the opposite stereochemistry vs. that observed experimentally assuming backside attack of malonate on the coordinated allyl fragment, thus raising the intriguing possibility that this reaction proceeds with retention of configuration. In addition, CO transfer was found to play a key role in the nucleophilic displacement reaction, giving as a product the tetracarbonylmolybdate complex **14**. This observation suggests that tricarbonylmolybdenum allyl species are key reactive intermediates in the catalytic cycle.

REFERENCES

1. (a) B. M. Trost and D. L. van Vranken. *Chem. Rev.* **96**, 395 (1996); (b) T. Hayashi. In *Catalytic Asymmetric Synthesis*, I. Ojima (Ed.), pp. 325–365, VCH, New York (1993); (c) G. Consigio and R. M. Waymouth. *Chem. Rev*. **89**, 257 (1989).
2. G. C. Lloyd-Jones and A. Pfaltz. *Angew. Chem., Int. Ed. Engl*. **34**, 462–464 (1995).
3. (a) B. M. Trost and I. Hachiya. *J. Am. Chem. Soc.* **120**, 1104–1105 (1998); (b) B. M. Trost, S. Hildbrand, K. Dogra. *J. Am. Chem. Soc.* **121**, 10416–10417 (1999).
4. (a) A. V. Malkov, P. Spoor, V. Vinader, P. Kočovský. *Tetrahedron. Lett.* **42**, 509–512 (2001); (b) P. Kočovský, A. V. Malkov, S. Vyskočil, G. C. Lloyd-Jones. *Pure Appl. Chem.* **71**, 1425–1433 (1999).
5. (a) F. Glorius and A. Pfaltz. *Org. Lett.* **1**, 141–144 (1999); (b) F. Glorius, M. Neuburger, A. Pfaltz. *Helv. Chim. Acta* **84**, 3178–3196 (2001).
6. (a) N.-F. K. Kaiser, U. Bremberg, M. Larhed, C. Moberg, A. Hallberg. *Angew. Chem., Int. Ed. Engl.* **39**, 3596–3598 (2000); (b) O. Belda, N.-F. Kaiser, U. Bremberg, M. Larhed, A. Hallberg, C. Moberg. *J. Org. Chem.* **65**, 5868–5870 (2000).
7. M. Palucki, J. M. Um, N. Yasuda, D. A. Conlon, F.-R. Tsay, F. W. Hartner, Y. Hsiao, B. Marcune, S. Karady, D. L. Hughes, P. G. Dormer, P. J. Reider. *J. Org. Chem.* **67**, 5508–5516 (2002).
8. (a) B. M. Trost and K. Dogra. *J. Am. Chem. Soc.* **124**, 7256–7257 (2002); (b) B. M. Trost and N. G. Andersen. *J. Am. Chem. Soc.* **124**, 14320–14321 (2002).
9. M. Palucki, J. M. Um, D. A. Conlon, N. Yasuda, D. L. Hughes, B. Mao, J. Wang, P. J. Reider. *Adv. Synth. Catal* **343**, 46–50 (2001).
10. B. M. Trost, K. Dogra, I. Hachiya, T. Emura, D. L. Hughes, S. Krska, R. A. Reamer, M. P. Palucki, N. Yasuda, P. J. Reider. *Angew. Chem., Int. Ed. Engl.* **41**, 1929–1932 (2002).
11. D. Morales, J. Pérez, L. Riera, V. Riera, R. Corzo-Suárez, S. García-Granda, D. Miguel. *Organometallics* **21**, 1540–1545 (2002).
12. S. W. Krska, D. L. Hughes, R. A. Reamer, D. J. Mathre, Y. Sun, B. M. Trost. *J. Am. Chem. Soc.* **124**, 12656–12657 (2002).
13. M. D. Curtis and O. Eisenstein. *Organometallics* **3**, 887–895 (1984).

14. (a) B. M. Trost and P. E. Strege. *J. Am. Chem. Soc*. **97**, 2534 (1975); (b) B. M. Trost and T. R. Verhoeven. *J. Org. Chem*. **41**, 3215 (1976); (c) T. Hayashi, T. Hagihara, M. Knonishi, M. Kumada. *J. Am. Chem. Soc*. **105**, 7767 (1983); (d) T. Hayashi, M. Konishi, M. Kumada. *J. Chem. Soc., Chem. Commun*. 107 (1984); (e) T. Hayashi, A. Yamamoto, T. Hagihara. *J. Org. Chem*. **51**, 723 (1986); (f) P. B. Mackenzie, J. Whelan, B. Bosnich. *J. Am. Chem. Soc*. **107**, 2046–2054 (1985).
15. (a) J. W. Faller and D. Linebarrier. *Organometallics* **7**, 1670 (1988); (b) A. Rubio and L. S. Liebeskind. *J. Am. Chem. Soc*. **115**, 891–901 (1993); (c) A. Kuhl, J. A. Christopher, L. J. Farrugia, P. J. Kocienski. *Synlett* 1765–1768 (2000); (d) Y. D. Ward, L. A. Villanueva, G. D. Allred, L. S. Liebeskind. *J. Am. Chem. Soc*. **118**, 897–898 (1996).
16. D. Dvořák, I. Starý, P. Kočovský. *J. Am. Chem. Soc*. **117**, 6130–6131 (1995).
17. D. L. Hughes, M. Palucki, N. Yasuda, R. A. Reamer, P. J. Reider. *J. Org. Chem.* **67**, 2762–2768 (2002).